

Evaluating Noise Pulses in RC Networks due to Capacitive Coupling

Yehea I. Ismail
Electrical and computer Engineering Department
Northwestern University

Abstract - Closed form solutions are introduced that describe the area, width, and maximum value of a noise pulse induced on a quiet net (line, tree, or mesh) due to capacitive coupling with switching neighbor nets. These solutions are highly efficient to evaluate with a complexity linearly proportional to the number of elements in the RC network. The pulse area calculated based on these solutions is *exact* while the width and maximum value of the noise pulse are within 15% from SPICE simulations for a wide range of typical interconnect structures. The effects of the coupled line impedances and line length on the amount of noise induced on a quiet line are investigated based on these solutions. It is shown that the energy of a noise pulse is quadratic with the length of an interconnect line, illustrating the need for accurate noise estimation for large interconnects.

I. Introduction

Noise evaluation and reduction is becoming of crucial importance in current high performance integrated circuits. Coupling noise has dramatically increased with technology scaling due to higher operating frequencies, closer circuitry, increasing height of interconnect lines, and longer global wires. This increase in coupling noise was accompanied by a decrease in the noise immunity of CMOS circuits due to the scaling down of the supply voltage. Also, noise liable dynamic circuit families are increasingly being used in high performance integrated circuits due to their lower power consumption and higher performance as compared to static CMOS circuits. This two-fold effect of technology scaling has made noise a very important design parameter in current integrated circuits and the importance of noise will only increase in future generations of integrated circuits.

Some work in noise evaluation did not correctly interpret the relation between the moments and noise pulses *e.g.*, [1]-[3]. Hence, closed form solutions are introduced based on the first few moments of the transfer function at the node of interest in the victim net. The calculation of these moments is especially efficient for coupled RC trees and lines (with no resistive loops) requiring no matrix inversion and therefore has a linear complexity with the number of elements in the circuit [4]-[8]. Note that the overwhelming majority of on-chip interconnect belong to this category.

The paper is organized as follows. The closed form solutions to evaluate the area, width, and the maximum value of a noise pulse are presented in section II and are compared to SPICE simulations. The effects of the coupled line impedances, and line length on noise are investigated in section III. Conclusions are provided in section IV. Finally, the calculation of the response moments at different nodes of capacitively coupled trees using simple recursive formulae is illustrated in the Appendix.

II. Characterizing a Noise Pulse

A method is introduced in this section to efficiently determine the maximum value and width of a noise pulse with reasonable accuracy. The exact area under a noise pulse is characterized in subsection A. This area is used to determine the amplitude and width of a noise pulse on an RC network in subsection B.

A. Determining the Exact Area Under a Noise Pulse

A signal $V(s)$ at a certain node of an RC network that reaches a final value of m_0 can be expanded into a power series of s that is given by

$$V(s) = \frac{m_0}{s} + m_1 + m_2s + m_3s^2 + \dots, \quad (1)$$

where m_i is the i^{th} moment of the signal $V(s)$ [4]-[6]. The pole at $s = 0$ represented by the first term in (1) determines the final value of $V(s)$ since according to the final value theorem

$$\lim_{t \rightarrow \infty} v(t) = \lim_{s \rightarrow 0} [s \cdot V(s)] = m_0. \quad (2)$$

It will be assumed through out the paper that all the signals at the nodes of the aggressor nets rise to a final value of one and that the victim net is steady at zero volts. This case represents the worst case coupling noise. The results can later be scaled by the supply voltage V_{DD} . The noise pulse at a victim net tends to zero as time tends to infinity since the signals on the aggressor nets reach their steady state values (V_{DD} or GND) and the coupling capacitors and inductors appear as open and short circuits, respectively. Hence, the noise pulse at a victim node v , $E_v(s)$, is given by

$$E_v(s) = m_1 + m_2s + m_3s^2 + \dots, \quad (3)$$

with $m_0 = 0$ due to the zero final value of the noise pulse. The total area under the noise pulse A is given by

$$A = \int_{-\infty}^{\infty} e_v(t) dt. \quad (4)$$

Using the definition of the Laplace transform and expanding e^{-st} into powers of s , $E_v(s)$ can be expressed as

$$E_v(s) = \int_{-\infty}^{\infty} e_v(t) e^{-st} dt = \int_{-\infty}^{\infty} e_v(t) dt - \left[\int_{-\infty}^{\infty} e_v(t) t dt \right] s + \left[\int_{-\infty}^{\infty} e_v(t) \frac{t^2}{2} dt \right] s^2 + \dots \quad (5)$$

Comparing (3) to (5), the following relation results

$$A = \int_{-\infty}^{\infty} e_v(t) dt = m_1. \quad (6)$$

Hence, the total area under a noise pulse is equal to the first moment of the noise signal. Note that this relation is *exact*. The area of a noise pulse is by itself an important metric that can be used to characterize the noise pulse especially for RC circuits. The first moment of the noise signal can be calculated with high efficiency. For a tree structured interconnect with all the signals on the aggressor nets rising to one for worst case noise, the first moment at a victim node v is given by (See the appendix)

$$m_{1,v} = \sum_k C_{c\tau k} R_k, \quad (7)$$

where the summation index k operates over all of the resistors that belong to the path from the input to the victim node v . R_k is the resistance of section k while $C_{c\tau k}$ is the total coupling capacitance down stream of node k .

The area under the noise pulse depends only on the resistances of the victim net and the coupling capacitances to aggressor nets. It is shown in the appendix that the area does not depend on the characteristics of aggressor nets or the input waveform shapes of aggressor nets. Hence, the area under the noise pulse is an absolute characteristic of the victim net and the coupling capacitances. It is also shown in the appendix that the area under the noise pulse does not depend on the input rise time in the circuit. To illustrate this fact, the input signal to one of two capacitively coupled RC lines is kept constant at zero volts while the other line have an exponential signal at their input of the form

$$V_{in} = 1 - e^{-\frac{t}{T}}, \quad (8)$$

where T is the time constant of the exponential and determines the rise time of the input signal $t_{rn} = 2.3T$. The induced noise pulse at the victim node is simulated using SPICE for several input rise times. The simulation results are depicted in Fig. 1. Note that despite the change in the pulse shape, the total area under the pulse remains constant.

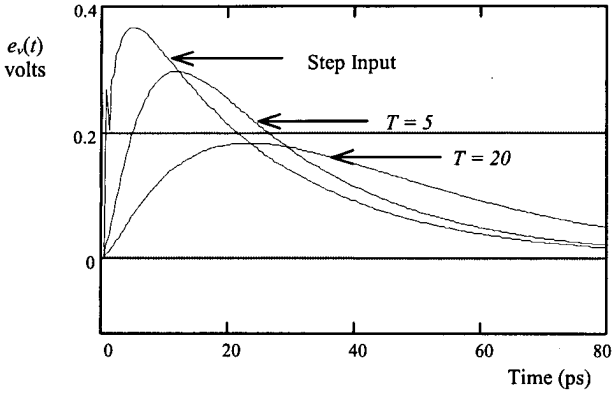


Fig. 1. Noise pulses at the end of one of two coupled RC lines for different aggressor input rise times. Note that the area under the noise pulses is not affected by the input rise time.

B. Characterizing the Amplitude and Width of a Noise Pulse

The area under a noise pulse can be used to calculate the amplitude of the pulse if the pulse width is known. To calculate the width of a noise pulse, the noise signal at node v is approximated by the first order response given by

$$\tilde{E}_v(s) = \frac{m_1}{1 + \left[-\frac{m_2}{m_1} \right] \cdot s} \quad (9)$$

where m_1 and m_2 are the first and second moments of the noise pulse $E_v(s)$ as described by (3). By expanding $\tilde{E}_v(s)$ into powers of s , it can be verified that $\tilde{E}_v(s)$ matches the first two moments of the exact noise pulse $E_v(s)$. Note that the input waveform shapes to the aggressor nets are included in the calculation of m_2 as shown in the appendix. Calculating the inverse Laplace transform, the noise pulse in the time domain is given by

$$\tilde{e}_v(t) = -\frac{(m_1)^2}{m_2} \cdot \exp\left(\frac{m_1}{m_2} \cdot t\right) \quad (10)$$

Referring to (3) and (5) and noting that $e_v(t)$ is positive for all t , m_1 and m_2 are guaranteed to have inverse signs. This fact guarantees the stability of the approximate response.

The approximate signal $\tilde{e}_v(t)$ results in a significant error at $t = 0$ and instead of satisfying the zero initial conditions, $\tilde{e}_v(t)$ has an initial value given by $-(m_1)^2/m_2$. This initial error is because one exponential cannot represent the rising and falling parts of a noise pulse. At least two exponentials are required to describe the entire noise pulse which requires a second order system. However, the information around $t = 0$ is not required to determine the width of the noise pulse since the pulse is known to start at $t = 0$. It is only required to determine the time at which the noise pulse ends. The actual time required for the pulse to return to zero is infinite. Hence, a cutoff time should be selected such that most of the pulse energy is concentrated before this time. This cutoff time is arbitrarily chosen here at the instant when $\tilde{e}_v(t)$ falls to 10% of its initial value. Therefore, the width of the pulse w can be calculated from (10) as

$$w = \ln(0.1) \cdot \frac{m_2}{m_1} \quad (11)$$

The above relation estimates the noise pulse width with high accuracy. This claim can be justified by noting that $\tilde{E}_v(s)$ accurately represents the exact

response $E_v(s)$ around $s = 0$ (i.e., when s is small) since the terms with higher powers of s in the series expansion (3) become negligible. The region where s is small maps in the time domain to the time when the noise pulse approaches its steady state. Hence, the approximation in (10) is particularly accurate towards the end of the noise pulse, which is the region of most interest when determining the pulse width. For example, consider the three coupled transmission lines shown in Fig. 2. The input signal to line two is kept constant at zero volts while lines one and three have unit step signals at their inputs. The induced noise pulse at the end of line two is simulated using SPICE and the result is compared to (10) in Fig. 3. Note that (10) accurately matches SPICE simulations towards the end of the noise pulse.

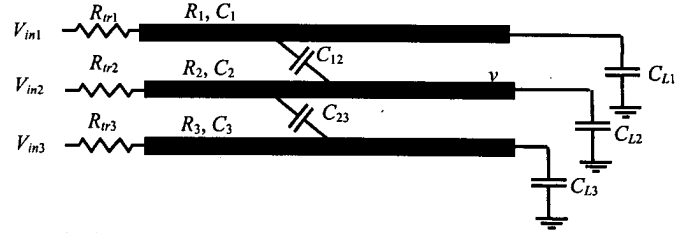


Fig. 2. Three capacitively coupled RC transmission lines.

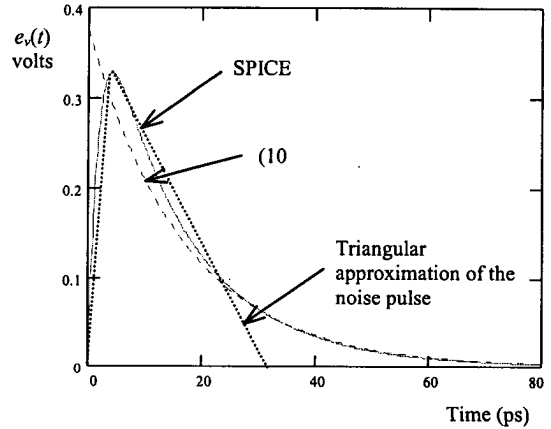


Fig. 3. (10) as compared to SPICE.

To determine the amplitude of the noise pulse, the pulse can be approximated by a triangle whose base is w and area is A as shown in Fig. 3. Based on this approximation, the amplitude of the noise pulse e_{max} can be calculated from

$$e_{max} = 2 \frac{A}{w} = \frac{2}{\ln(0.1)} \cdot \frac{(m_1)^2}{m_2} \quad (12)$$

Alternatively, a parabola that has an area A and zeros at $t = 0$ and $t = w$ can be used to approximate the noise pulse. This parabola is given by

$$\tilde{e}_v(t) = 6 \frac{A}{w^3} \cdot t \cdot (w - t) \quad (13)$$

The maximum value according to this approximation is given by

$$e_{max} = \frac{3}{2} \frac{A}{w} = \frac{3}{2 \ln(0.1)} \cdot \frac{(m_1)^2}{m_2} \quad (14)$$

Note that the amplitude of the noise pulse has the same dependence on the moments whether a first or a second order polynomial is used to approximate the pulse and the error is within a constant. The constant that

minimizes the error as compared to SPICE simulations is empirically determined and is around 0.84. Hence, the amplitude of the noise pulse is given by

$$e_{\max} = -0.84 \cdot \frac{(m_1)^2}{m_2} \quad (15)$$

Since the area of the noise pulse is exact and the pulse width is estimated with high accuracy, the pulse amplitude as described by (15) is expected to be acceptably accurate. The amplitude and width of a noise pulse estimated using (11) and (15) are compared to SPICE in Table 1 for the three coupled transmission lines shown in Fig. 2 with different line impedances, coupling capacitances, and inputs to the lines one and three. The expressions given by (11) and (15) are within 10 percent from SPICE for a wide range of line impedances and input rise times. In general, (11) and (15) are within 20 percent from SPICE for a wide range of typical interconnect structures.

Table 1. (11) and (15) as compared to SPICE for node v in the circuit shown in Fig. 2. The circuit element values are: $R_1=2$, $C_1=2$, $R_{r1}=1$, $C_{L1}=1$, $R_2=0.5$, $C_2=0.5$, $R_{r2}=0.5$, $C_{L2}=0.5$, $R_3=2$, $C_3=2$, $R_{r3}=1$, $C_{L3}=1$, $C_{12}=1$, and $C_{23}=1$. Only the changes from these values are listed in the table. Resistances are in ohms and capacitances are in pF.

Changes in circuit Parameters	w SPICE (ps)	(11) (ps)	% error	e_{\max} SPICE volts	(15) volts	% error
No change	21.5	21.79	1.1%	0.136	0.141	4.3%
$C_{23}=2$	25.6	25.8	0.7%	0.171	0.176	2.9%
$C_{12}=2$ $C_{23}=2$	28.6	28.63	0.1%	0.208	0.216	3.9%
$R_3=4$ $C_3=1.5$	24.0	24.02	0%	0.1279	0.1288	0.7%
$R_2=4$ $C_2=1$	24	23.9	0.4%	0.137	0.129	5.4%
$R_2=1$ $C_2=1$	24.73	24.8	0.3%	0.155	0.167	7.7%
$R_2=4$ $C_2=4$	50.8	51.5	0.13%	0.19	0.204	7.6%
$t_{rin}=7$ ps	27.9	28.6	2.5%	0.103	0.107	4.3%
$t_{rin}=15$ ps	35	36.5	4.1%	0.079	0.084	7.2%

III. Effects of the Interconnect Parameters on Coupling Noise

The expressions for A , w , and e_{\max} developed in section II can be computed in closed form for the special case of a set of coupled transmission lines. Although, the conclusions made in this section are for the special case of two coupled transmission lines, most of the intuitive remarks apply to the general case of capacitively coupled RC trees and meshes. Consider a two coupled RC lines with length l . Line one has a resistance and capacitance per unit length of R_1 and C_1 while line two has a resistance and capacitance per unit length of R_2 and C_2 . The two lines are coupled by a capacitance of C_{12} per unit length. Line two has a unit step input while the input to line one remains constant at zero volts. It can be shown that the first two moments of the transfer function at the end of line one are given by (See the appendix)

$$m_1 = R_1 C_{12} \frac{l^2}{2} = A, \quad (16)$$

$$m_2 = -R_1 C_{12} \frac{l^4}{8} [R_1 (C_1 + C_{12}) + R_2 (C_2 + C_{12})], \quad (17)$$

respectively. The width and amplitude of the noise pulse can be calculated from (11) and (15), respectively, and are given by

$$w = 0.576 \cdot l^2 [R_1 (C_1 + C_{12}) + R_2 (C_2 + C_{12})], \quad (18)$$

$$e_{\max} = \frac{1.68 \cdot R_1 C_{12}}{[R_1 (C_1 + C_{12}) + R_2 (C_2 + C_{12})]}, \quad (19)$$

The effect of increasing the length of the two wires is to slow down the signal on line two (the aggressor) since the delay and rise time of the output signal at the end of an RC transmission line is quadratically dependent on the length of the line [9]. Current is injected into line one via the coupling capacitance until the signal at line two approaches its steady state, which explains the quadratic increase in the pulse width with the length of the lines. The amplitude of the pulse, however, is not affected by the line lengths. The signal on line two slows down quadratically with the length of the lines, which quadratically reduces the current injected into line one via coupling capacitance since the injected current is proportional to the switching speeds of the signals on the aggressor nets. However, the total coupling capacitance increases linearly with the length and so does the total resistance of line one. Thus, the quadratic effect of increased C_{12} and R_1 cancels the quadratic slow down of the signal on line two and the amplitude of the noise pulse remains constant. The total area of the noise pulse given by (16) represents the total energy of the noise pulse and increases quadratically with the interconnect length primarily because of the increase in the pulse width. Hence, the effect of the interconnect length on coupling noise is profound with longer lines (or in general larger interconnects) suffering much more coupling noise as compared to shorter lines.

Another interesting observation is that the energy of the noise pulse in (16) does not depend on the parameters of line two (the aggressor line). This trend can be explained by noting that if the parameters of line two change such that the signals on line two become slower, the amplitude of the noise pulse on line one decreases while its width increases. These two opposite effects cancel and the area of the noise pulse remains constant. Mathematically, (18) and (19) illustrate this trait with the effect of R_2 and C_2 canceling when multiplying the two equations. An increase in the coupling capacitance per unit area C_{12} slows the signal on line two which increases the width of the noise pulse as illustrated by (18). Also, the increase in C_{12} increases the injected current into line one which partially cancels the effect of slower aggressor signal on the pulse amplitude. This trait explains the weak dependence of the amplitude e_{\max} on C_{12} in (19). The area of the noise pulse is proportional to the product of the pulse amplitude and width and is therefore proportional to C_{12} . Hence, the general statement can be made that the width and area of a noise pulse increases linearly as the coupling capacitance per unit length increases while the pulse amplitude increases slowly with increasing the coupling capacitance.

Increasing the resistance and capacitance of the victim line R_1 and C_1 increases the pulse width. This effect is evident in the time constant term $R_1(C_1+C_{12})$ in (18). This term represents the time needed to discharge the voltages accumulated on the capacitors of the victim line during the switching of the aggressor line. If this time constant is significantly larger than the time constant of the aggressor net, the pulse width may be significantly wider than the switching time of the aggressor nets. The effect of the capacitance to ground of the victim net is to decrease the amplitude of the noise pulse since a larger C_1 charges to a lower voltage given the same amount of injected current via coupling capacitances. The increase in pulse width is cancelled by the decrease in the pulse amplitude when increasing the capacitance of the victim net and the pulse area is independent of the victim net capacitance as illustrated by (16). Hence, the general statement can be made that wider lines (with sufficiently large capacitance to ground) suffer noise pulses with lower amplitudes as compared to narrow lines. If a line is sufficiently wide, the noise amplitude to this line can be kept below the receiver's threshold voltage which renders the noise pulse non-harmful.

A final observation is that the input waveform shapes on the aggressor nets does not affect the area under the noise pulse given by (16). Intuitively, if the inputs of the aggressor nets switch faster, the signals on the aggressor nets are faster. The amplitude of the noise pulse on the victim line increases due to the higher injected current via the coupling capacitances while the pulse width decreases due to the aggressor signals reaching their final value faster. These two opposite effects cancel and the area of the noise pulse remains constant.

IV. Conclusions

Closed form solutions were introduced that describe the area, width, and maximum value of a noise pulse induced on a quiet net due to

capacitive coupling with switching nets. These solutions are highly efficient with a complexity linearly proportional to the number of elements in the network. The width and maximum value of the noise pulse are within 15% from SPICE simulations for a wide variety of typical interconnect structures. The effects of the coupled line impedances and line length on the amount of noise induced on a quiet line were investigated. It was shown that the energy of a noise pulse is quadratic with the length of an interconnect line which illustrates the need for accurate noise estimation for large interconnects.

Appendix: Moments Calculation for Capacitively Coupled RC Trees

For any interconnect structure, if after removing the capacitive coupling all that remains is a set of RC trees and lines, this structure is considered a tree based structure. For such capacitively coupled RC trees, the moments of the response at different nodes can be calculated in linear time using simple recursive formulae. Capacitively coupled trees have multiple inputs. The case is considered here when all the inputs have the same waveform shape but are not necessarily switching in the same direction. The waveform shape is arbitrary. For a node i where the moments are being calculated, the input with a DC path to i is called the primary input.

Consider calculating the moments at node i of a capacitively coupled tree structure. The voltage at node i can be expressed as

$$V_i(s) = V_{inp}(s) - \sum_k \left[R_{ik} \sum_j C_{kj} s (V_k(s) - V_j(s)) \right], \quad (20)$$

where k runs over all the nodes in the same tree which i belongs to and j runs over all the nodes which k has a capacitance connected to. In the case of capacitances to ground, $j = 0$. V_{inp} is the primary input for node i . R_{ik} is the common resistance from the input to the nodes i and k . The above formula can be understood by noting that the summations

$$\sum_j C_{kj} s (V_k(s) - V_j(s)) \quad (21)$$

represent the currents flowing out of node k . The term

$$R_{ik} \sum_j C_{kj} s (V_k(s) - V_j(s)) \quad (22)$$

in (17) represents the voltage drop between the primary input and node i due to the current flowing out of node k . Note that the node k belongs to the same tree as i since it is this current that has to run through R_{ik} .

By expanding the voltages in (20) into powers of s given by

$$\begin{aligned} V_i(s) &= \frac{m_{0,i}}{s} + m_{1,i} + m_{2,i}s + m_{3,i}s^2 + \dots \\ V_{inp}(s) &= \frac{m_{0,inp}}{s} + m_{1,inp} + m_{2,inp}s + m_{3,inp}s^2 + \dots \\ V_k(s) &= \frac{m_{0,k}}{s} + m_{1,k} + m_{2,k}s + m_{3,k}s^2 + \dots \\ &\vdots \end{aligned} \quad (23)$$

and comparing similar powers of s on both sides of (20), the following relations result

$$\begin{aligned} m_{0,i} &= m_{0,inp} \\ m_{n,i} &= m_{n,inp} - \sum_k \left[R_{ik} \sum_j C_{kj} (m_{n-1,k} - m_{n-1,j}) \right] \quad \text{for } n = 1, 2, 3, \dots \end{aligned} \quad (24)$$

These relations allows calculating all the moments recursively in linear time. Note that the moments of the inputs are known since the inputs are given. For example, if the input signal is given by

$$V_{inp} = 1 - e^{-\frac{t}{T}}, \quad (25)$$

the moments are given by $m_{0,inp} = 1$, $m_{n,inp} = T^n$.

In the case considered in this paper where the moments are calculated at a victim node v on a quiet line with all other lines switching from low to high, the moments $m_{0,k} = 0$ at all the nodes belonging to the tree that v belongs to including v while $m_{0,j} = 1$ for all nodes belonging to other nets. Hence, by substituting in (24), the first moment at the victim node v is given by

$$m_{1,v} = \sum_k R_{v,k} \sum_j C_{kj} \quad \text{with } j \neq 0, \quad (26)$$

which can be put as

$$m_{1,v} = \sum_k C_{cTk} R_k, \quad (27)$$

where the summation index k operates over all of the resistors that belong to the path from the input to the victim node v . R_k is the resistance of section k while C_{cTk} is the total coupling capacitance down stream of node k . Also, in the case of transmission lines, the summations in (24) become integrations and the moments can be calculated in closed form. In the case of two parallel coupled RC transmission lines, the moments on the quiet line due to the other line switching from low to high are given by

$$m_1 = R_1 C_{12} \frac{l^2}{2}, \quad (28)$$

$$m_2 = -R_1 C_{12} \frac{l^4}{8} [R_1 (C_1 + C_{12}) + R_2 (C_2 + C_{12})], \quad (29)$$

where l is the length of the two lines.

References

- [1] K. L. Shepard, V. Narayana, and R. Rose, "Harmony: Static Noise Analysis of Deep Submicron Digital Integrated Circuits," *IEEE Transactions on Computer-Aided Design*, Vol. 18, No. 8, pp. 1132 - 1150, August 1999.
- [2] A. Vittal and M. M. Sadowska, "Crosstalk Reduction for VLSI," *IEEE Transactions on Computer-Aided Design*, Vol. 16, No. 3, pp. 290 - 298, March 1997.
- [3] A. Devgan, "Efficient Coupled Noise Estimation for On-Chip Interconnects," *Proceedings of the IEEE/ACM International Conference on Computer-Aided Design*, September 1997.
- [4] L. T. Pillage and R. A. Rohrer, "Delay Evaluation with Lumped Linear RLC Interconnect Circuit Models," *Proceedings of the Caltech Conference on VLSI*, pp. 143-158, May 1989.
- [5] L. T. Pillage, R. A. Rohrer, and C. Visweswariah, *Electronic Circuit and System Simulation Methods*, McGraw-Hill, Inc., USA, 1994.
- [6] L. T. Pillage and R. A. Rohrer, "Asymptotic Waveform Evaluation for Timing Analysis," *IEEE Transactions on Computer-Aided Design*, Vol. CAD-9, No. 4, pp. 352 - 366, April 1990.
- [7] C. L. Ratzlaff, N. Gopal, and L. T. Pillage, "RICE: Rapid Interconnect Circuit Evaluator," *Proceedings of the IEEE/ACM Design Automation Conference*, pp. 555 - 560, June 1991.
- [8] T. K. Tang and M. S. Nakhla, "Analysis of High-Speed VLSI Interconnects Using the Asymptotic Waveform Evaluation Techniques," *IEEE Transactions on Computer-Aided Design*, Vol. CAD-11, No. 3, pp. 341 - 352, March 1992.
- [9] T. Sakurai, "Approximation of Wiring Delay in MOSFET LSI," *IEEE Journal of Solid-State Circuits*, Vol. SC-18, No. 4, pp. 418 - 426, August 1983.
- [10] W. H. Hayt, Jr., *Engineering Electromagnetics*, McGraw-Hill, Inc., USA, 1981.